AIAA 80-1447R

Wave Dynamics of Unsteady Compressible Flow Networks

V.E. Haloulakos*
McDonnell Douglas Astronautics Company, Huntington Beach, Calif.

The wave dynamics of compressible flow networks are analyzed by a modularly constructed computer code. The model solves the basic unsteady fluid flow equations via the method of characteristics and accounts for friction, heat transfer, and energy dissipation. Modules allow for constant and/or variable area ducts, moving pistons, and such boundary conditions as tees, crosses, open and closed ends, step area changes, variable area orifices, valves, thrusters, solid-propellant gas generators, finite, and infinite reservoirs. By judicious selection and numbering of modules the physical configuration of any flow network can be simulated. The code has played an instrumental role in the resolution of critical problems in connection with gas attitude control systems for missiles and spacecraft, airplane compartment decompressions, high-pressure waves in turbofan engines, and sound pressure waves in tube-launched missiles. Excellent correlation between predictions and test data was obtained.

Nomenclature

A,B = Riemann invariants
a = sonic velocity
c_p = specific heat at constant pressure
c_v = specific heat at constant volume
E = energy
E_f = energy dissipation function
f_i = body force
F_f = friction force
h = internally generated heat
p = pressure
q_i = heat flux
R = gas constant
s = entropy
S = flow area
t = time
T = temperature
u = fluid velocity
x = space variable
α,β = right and left running characteristics
γ = specific heat ratio
δ_{ij} = Kronecker delta
σ_{ij} = stress tensor ($\sigma_{ij} = -p\delta_{ii} + \tau_{ij}$)
τ_{ij} = shear stress tensor
ϕ = special function

All units are in lb, ft, s, °R

Introduction

THIS paper describes an unsteady compressible flow program[1] that contains the necessary flexibility for a wide range of applications and has been successfully used and verified in a number of cases, three of which are described herein.

The computational scheme uses the basic equations of unsteady compressible fluid flow, and the solution is obtained via the method of characteristics. The equations account for friction, heat transfer, and energy dissipation (or addition) effects. The computer program is modularly constructed permitting gas flow systems with almost any configuration to be analyzed. Modules can account for constant and/or variable area ducts, moving pistons, and such boundary conditions as tees, crosses, open and closed ends, step area changes, variable area orifices, valves, thrusters, solid-propellant gas generators, and infinite and finite reservoirs. By judicious selection and numbering of modules, the physical configuration of any flow network can be simulated.

Presented as Paper 80-1447 at the AIAA 13th Fluid and Plasma Dynamics Conference, Snowmass, Colo., July 14-16, 1980; submitted Sept. 11, 1980, revision received Feb. 27, 1981.

*Senior Scientist, Propulsion Department. Associate Fellow AIAA.

General Program Features

This section provides a brief description of the general features of the program. It includes the basic mathematical characteristics, the system elements and their boundaries, and the method used to interconnect elements and boundaries in constructing networks simulating the fluid flow systems.

Analytical Formulation

The mathematical formulation begins with the writing of the general conservation equations of a fluid followed by the customary assumptions applicable to the specific problem under consideration.

The basic equations of motion are

Continuity

$$\frac{\partial}{\partial t}(\rho S) + \frac{\partial}{\partial x_i}(\rho S u_i) = 0 \tag{1}$$

Momentum

$$\rho\left(\frac{\partial u_i}{\partial t} + u_j\frac{\partial u_i}{\partial x_j}\right) = \rho f_i + \frac{\partial \sigma_{ij}}{\partial x_j} \tag{2}$$

Energy

$$\rho\frac{dE}{dt} = \sigma_{ij}\frac{\partial u_i}{\partial x_j} + \frac{\partial q_i}{\partial x_i} + \rho h \tag{3}$$

State

$$p = \rho RT \tag{4}$$

Assumptions

1) Variable area rigid duct.
2) No body forces.
3) One-dimensional flow.
4) Viscous fluid.
5) No internally generated heat.
6) Constant specific heats and molecular weight.

Introducing these assumptions, the basic equations become

$$\frac{\partial \rho}{\partial t}+u\frac{\partial \rho}{\partial x}+\rho\frac{\partial u}{\partial x}+\frac{\rho}{S}\left(\frac{\partial S}{\partial t}+u\frac{\partial S}{\partial x}\right)=0 \tag{5}$$

$$\frac{\partial u}{\partial t}+u\frac{\partial u}{\partial x}+\frac{1}{\rho}\frac{\partial p}{\partial x}+F_f=0 \tag{6}$$

$$\left(\frac{\partial \rho}{\partial t}+u\frac{\partial p}{\partial x}\right)-a^2\left(\frac{\partial \rho}{\partial t}+u\frac{\partial \rho}{\partial x}\right)-(\gamma-1)\left[\frac{\partial q}{\partial x}+E_f\right]=0 \tag{7}$$

$$p=\rho RT \tag{8}$$

A solution by the method of characteristics leads to

$$\left[\frac{\partial p}{\partial t}+(u\pm a)\frac{\partial p}{\partial x}\right]\pm a\rho\left[\frac{\partial u}{\partial t}+(u\pm a)\frac{\partial u}{\partial x}\right]$$

$$\pm aF_f-(\gamma-1)\left[\frac{\partial q}{\partial x}+E_f\right]+\frac{\rho a^2}{S}\left[\frac{\partial S}{\partial t}+u\frac{\partial S}{\partial x}\right]=0 \tag{9}$$

which results in the following set of equations:

$$\frac{\mathrm{d}p}{\mathrm{d}t}+a\rho\frac{\mathrm{d}u}{\mathrm{d}t}+a\rho F_f-(\gamma-1)\left(\frac{\partial q}{\partial x}+E_f\right)+\frac{\rho a^2}{S}\frac{\mathrm{d}S}{\mathrm{d}t}=0 \quad \text{along} \quad \frac{\mathrm{d}x}{\mathrm{d}t}=u+a \tag{10}$$

$$\frac{\mathrm{d}p}{\mathrm{d}t}-a\rho\frac{\mathrm{d}u}{\mathrm{d}t}-a\rho F_f-(\gamma-1)\left(\frac{\partial q}{\partial x}+E_f\right)+\frac{\rho a^2}{S}\frac{\mathrm{d}S}{\mathrm{d}t}=0 \quad \text{along} \quad \frac{\mathrm{d}x}{\mathrm{d}t}=u-a \tag{11}$$

and finally

$$\frac{\mathrm{d}p}{\mathrm{d}t}-a^2\frac{\mathrm{d}\rho}{\mathrm{d}t}-(\gamma-1)\left(\frac{\partial q}{\partial x}+E_f\right)=0 \quad \text{along} \quad \frac{\mathrm{d}x}{\mathrm{d}t}=u \tag{12}$$

If the heat transfer and energy dissipation functions are expressed on per-unit-mass basis and if the pressure is expressed in terms of the density and entropy, Eq. (12) becomes

$$\frac{\mathrm{d}s}{\mathrm{d}t}=\frac{R\rho}{p}\left[\frac{\partial q}{\partial x}+E_f\right] \tag{13}$$

which represents a continuous variation in entropy along the fluid streamlines.

Introducing a new function ϕ such that

$$\mathrm{d}\phi=\frac{\mathrm{d}p}{\mathrm{d}\rho}+C\mathrm{d}s \tag{14}$$

and utilizing the basic thermodynamic relationships

$$p=f(s)\rho^{\gamma} \tag{15}$$

$$\mathrm{d}s=c_v\frac{\mathrm{d}T}{T}-R\frac{\mathrm{d}\rho}{\rho} \tag{16}$$

Eqs. (10) and (11) become

$$\mathrm{d}A=G\mathrm{d}t+C\mathrm{d}s \quad \text{for} \quad \mathrm{d}x=\alpha\mathrm{d}t \tag{17}$$

$$\mathrm{d}B=N\mathrm{d}t+C\mathrm{d}s \quad \text{for} \quad \mathrm{d}x=\beta\mathrm{d}t \tag{18}$$

where

$$G=-F_f+\frac{\gamma-1}{a}\left(\frac{\partial q}{\partial x}+E_f\right)-\frac{a}{S}\frac{\mathrm{d}S}{\mathrm{d}t} \tag{19}$$

$$N=F_f+\frac{\gamma-1}{a}\left(\frac{\partial q}{\partial x}+E_f\right)-\frac{a}{S}\frac{\mathrm{d}S}{\mathrm{d}t} \tag{20}$$

$$C=a/c_p(\gamma-1) \tag{21}$$

$$\phi=[2/(\gamma-1)]a \tag{22}$$

$$A=\phi+u \tag{23}$$

$$B=\phi-u \tag{24}$$

$$\alpha=u+a \tag{25}$$

$$\beta=u-a \tag{26}$$

Computation Procedure

Equations (13), (17), and (18) form the basis of the computation technique by utilizing the characteristic grid shown in Fig. 1 and computing the various coefficients via Eqs. (19-26). A set of initial conditions are input along the entire boundary, i.e., for all values of x the flow is completely specified, and via the use of the above-cited equations, a new set of flow parameters is computed a time step Δt later. The program uses interpolation routines to obtain the values of the flow variables at the stations x_α, x_u, and x_β via the use of the data at the adjacent points, x_{i-1}, x_i, and x_{i+1}. The entropy increase is calculated along the steamline and the remaining of the flow variables are computed along the α- and β-characteristics. The net of selected characteristics has the good features of quick convergence and an effective way of handling multiple ducts and the various boundary conditions imposed on the flow by the system geometry. Futhermore, it

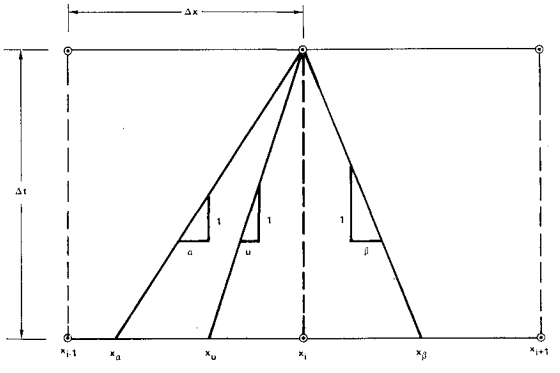

Fig. 1 Basic characteristics computation grid net.

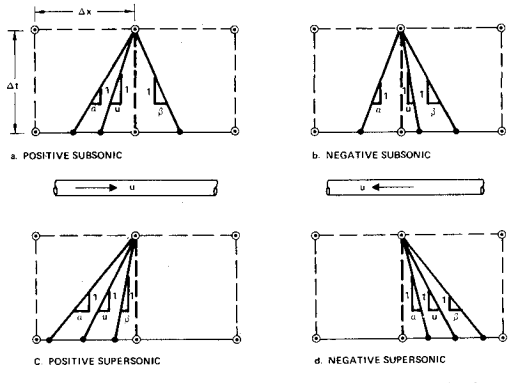

Fig. 2 Characteristic grids for various flowfields.

Table 1 Computer-constructed configuration tree

Section	Zero end	One end	Connections		Valve no.
1	Gas generator	Area change	2		
2	Area change	Cross	3	4	
3	Cross	Valve			1
4	Cross	Cross	5	10	
5	Cross	Cross	6	7	
6	Cross	Valve			2
7	Cross	Cross	8	9	
8	Cross	Valve			3
9	Cross	Dead end			
10	Cross	Cross	11	12	
11	Cross	Valve			4
12	Cross	Cross	13	14	
13	Cross	Valve			5
14	Cross	Cross	26	27	
15	Gas generator	Area change	16		
16	Area change	Cross	17	18	
17	Cross	Valve			6
18	Cross	Cross	19	24	
19	Cross	Cross	20	21	
20	Cross	Valve			7
21	Cross	Cross	22	23	
22	Cross	Valve			8
23	Cross	Dead end			
24	Cross	Cross	25	26	
25	Cross	Valve			9
26	Cross	Cross	14		
27	Cross	Valve			10

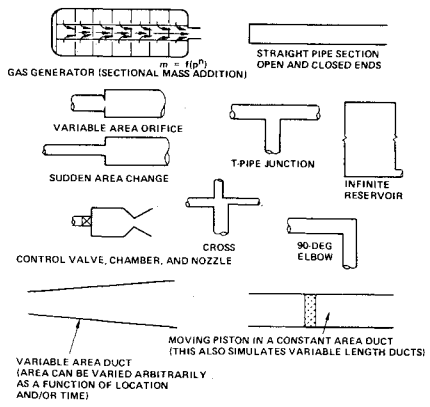

Fig. 3 Basic elements and boundaries.

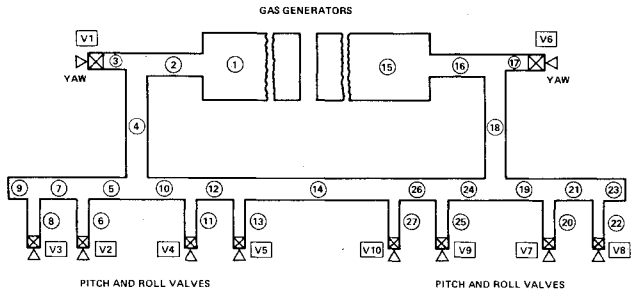

Fig. 4 Hot-gas control system configuration.

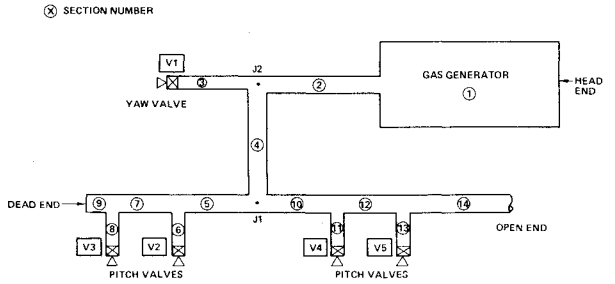

Fig. 5 UpSTAGE hot-gas control system.

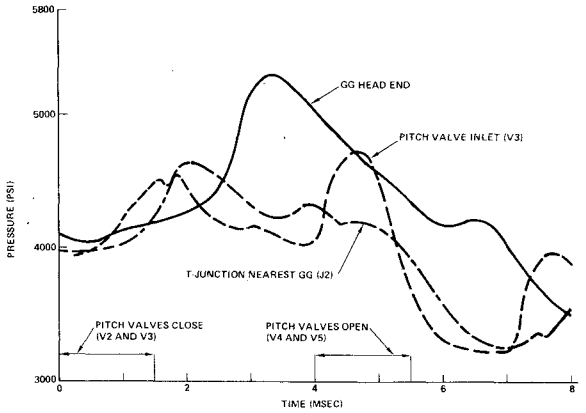

Fig. 6 UpSTAGE control system pressure transients.

can handle with equal ease and efficiency positive, negative, subsonic, or supersonic flows; the variations in the basic net are shown in Fig. 2 which simply indicates that the points x_u, x_α, and x_β are affected. The possibility of any of the points x_u, x_α, or x_β falling outside the prescribed space interval is precluded by the use of the "Courant-Friedrichs-Lewy" stability criteria which simply state that no wave travels more than Δx in any given Δt; which mathematically is given by

$$\Delta t \leq \Delta x / (|u| + a) \tag{27}$$

The actual procedure is to firmly establish the space increment Δx, enter an estimated Δt, and allow the program to change it if it is deemed necessary as dictated by the maximum values of the flow velocity u and the sonic velocity a. The basic elements and boundaries that give this program its complete geometric flexibility are shown in Fig. 3. Figure 4 shows a typical flow network containing most of these basic elements and boundaries interconnected and labeled representing a hot-gas control subsystem. Gas flow supplied by the gas generators is channeled and diverted throughout the system as the flow conditions warrant. As the valves open and close arbitrarily and independently, like a piano keyboard, the program computes the generation, transmission, reflection, and general behavior of all pressure waves. The transformation of this network into a computerized configuration tree is shown in Table 1.

Applications

The computer program has been used successfully in the resolution of numerous design and operational problems. For each of the three selected applications, this section provides a brief description of the problem, a set of key figures showing simulation and test data, and a summary of the contributions of the program to the resolution of the problem.

UpSTAGE Missile Control System

Problem

The problem on the UpSTAGE missile control system was to calculate the internal flow transients caused by the rapid closing and opening of the hot-gas control valves.

Simulation and Test Data

Figure 5 represents a schematic of one-half of the UpSTAGE hot gas control system; the other half is an exact mirror image. Figure 6 shows a set of typical pressure tran-

Table 2 Data correlation for the UpSTAGE hot gas control system[a]

Case	Ref pressure (P), psia		Pressure pulse (ΔP), psia		Correlation ($\Delta P/P$)	
	Simulation	Experiment	Simulation	Experiment	Simulation	Experiment
1	2700	2960	+1380	+1490	0.511	0.504
2	2900	3000	+891	+920	0.3072	0.3067

[a] Note: Gas source, solid-propellant gas generator; gas temperature, 3100°R or 2640°F; $+\Delta P$ is compression.

Table 3 Data correlation for the Skylab cold gas ACS[a]

Case	Ref pressure (P), psia		Pressure pulse (ΔP), psia		Correlation ($\Delta P/P$)	
	Simulation	Experiment	Simulation	Experiment	Simulation	Experiment
1	3200	3200	−580	−550	0.1809	0.1776
2	3200	3200	−690	−675	0.2153	0.2106
3	3200	3200	−860	−826	0.2683	0.2574

[a] Note: Gas source, high-pressure GN_2; gas temperature, 530°R or 70°F; $-\Delta P$ is expansion or rarefaction.

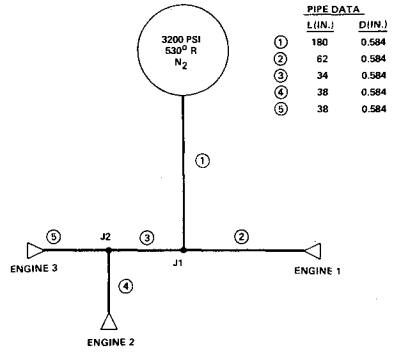

Fig. 7 Skylab ACS schematic.

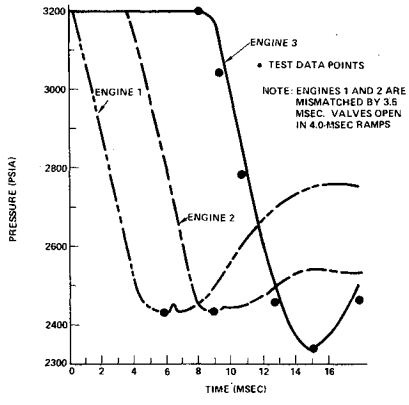

Fig. 8 Skylab ACS test data correlation.

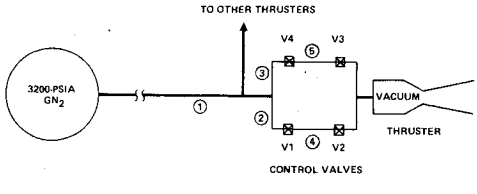

Fig. 9 Skylab ACS engine module schematic.

sients in the ducts and the gas generator as a result of closing the pitch control valves V2 and V3 and opening of valves V4 and V5. The rapidity with which the pressure in the gas generator goes from 4000 to 5300 psia should be noted. A representative comparison between the pressure data predicted by the program computations and those obtained by test is shown in Table 2.

Problem Resolution

By simulating a variety of critical operating conditions, the flow transients were charted, the peak pressure loads were established, and the proper safety factors were incorporated in the system design. The vehicles incorporating these designs were flown successfully and the control system worked flawlessly.

Skylab Attitude Control System

Problem

The problem in the Skylab Attitude Control System (ACS) was the "flow starving" of certain control system legs which was caused by the opening of control valves in adjacent engines or control modules. This resulted in either insufficient thrust from some of these engines or damaged control valves caused by excessive reverse pressure loads.

Simulation and Test Data

Figure 7 shows the ACS schematic, the piping dimensions, and the initial storage pressure. The opening of Engines 1 and 2 could be phased to completely drain leg ⑤ leading to Engine 3. This made it impossible for Engine 3 to generate full thrust when it was subsequently commanded open. Figure 8 shows the test and simulation data correlation obtained.

The details of control valve arrangement for each engine are shown in Fig. 9. Note the appropriate redundancy for maximum reliability against "valve closed" and/or "valve open" failure modes. Operating the engine by opening control valves V1 and V3, while control valves V3 and V4 remain closed, the pressure at the inlet of valve V4 drops as a result of the transient mass flow demand. If high pressure is trapped in leg ⑤, which is very likely, then control valve V4 experiences a very high reverse pressure. This happened in one of the routine tests and it was followed by the immediate destruction of the valve seat and a failure of the system. Numerous special tests were subsequently conducted to define the problem and also compare the test data with the results obtained from the program simulation. The close correlation is shown in Table 3.

Problem Resolution

The correct diagnosis of the control valve failure mechanism became possible only after the analysis using this computer program. The fluid transient phenomena were addressed and the resulting instantaneous pressure drops that caused the valve failures were found to be excessive ($\Delta P \sim 1100$ psi). When the feedline diameters were enlarged, as dictated by the results of the simulations, the pressure drops were reduced to approximately 300 psi, which were also predicted by the simulation. The system was tested and its integrity verified. This final design was flown in the Skylab and performed flawlessly.

Airplane Compartment Decompressions

Problem

Pressurized compartments of high-flying aircraft could decompress rapidly as a result of some sudden opening. As the size of these compartments becomes larger, transient fluid mechanics analysis must be used to analyze the phenomena. If multiple compartments are considered, the possibility of differential decompression exists, which may result in excessive structural loading on the partitions separating the compartments.

Simulation and Test Data

The program was used in such analyses, and it was compared with ground test data for both the single- and the multiple-compartment cases. Figure 10 shows the data for both simulation and test for a single compartment; the close correlation is evident.

The use of the program was expanded to simulate the case of multiple compartments. Figure 11 shows the geometry of a typical case with the partitions and vent geometry, which enhance the flow communications between compartments and serve to equalize the pressure on both sides of the partition, thus minimizing or eliminating any structural loads. As section (13) is opened in a 140-ms ramp, the flow transients cause each compartment to decompress differently. Figure 12 shows the pressure loads at the midpoint of the partition separating sections (2) and (4) following a multiple-compartment ground test. Similar, but not identical, data were obtained for several other points along the partition. The close correlation in both the magnitude of the peaks and the general shape of the transient curve between test and simulation should be noted. Simulation results are also shown for a set of pressure conditions corresponding to an altitude of 23,000 ft which could represent an airplane cruising altitude. The validity of the high-altitude simulations are ensured by the close correlation between test and simulation under ground conditions.

Problem Resolution

The correlations between test and simulation results in the cited cases render this program a valuable tool for design studies. In particular, its ability to assess the transients at altitude, based on ground test data, allows designs to be finalized without the need of decompression tests at high altitudes with actual airplanes.

Other Applications

The program has also been used in two other distinct problem areas.

1) The evaluation of strong pressure wave phenomena in turbofan engines caused by compressor stalls and/or explosions following fuel ingestion.

2) The calculation of sound pressure levels (SPL) associated with the firing of antitank missiles.

Excellent correlation was obtained in both cases; the details will be reported in a future paper.

Conclusions

The applicability of this program to a wide variety of unsteady flow problems has been demonstrated. Its configurational flexibility and computing scheme make it a valuable design tool for any system where compressible fluids flow through ducts and associated control components. It can identify and assess problem areas in candidate designs before any actual design is initiated. It can be used in lieu of hardware testing to evaluate candidate systems and also to extrapolate design data from one system to another. In fact, it gives far more information than tests do; e.g., data on flow velocity, density, etc. are not easily obtainable from tests. Judicious use of this program can identify the most viable and promising designs which can be subjected to testing, if necessary. This can result in substantial cost savings.

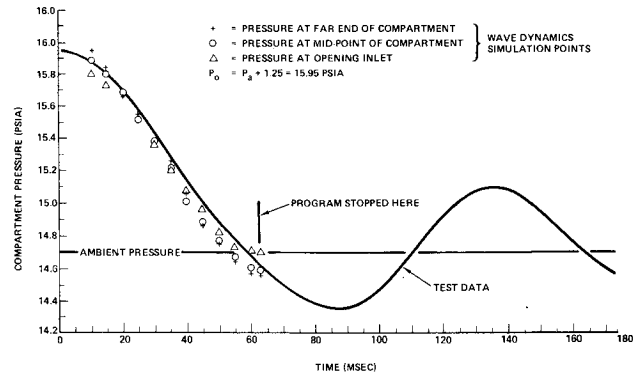

Fig. 10 Single test compartment decompression transients.

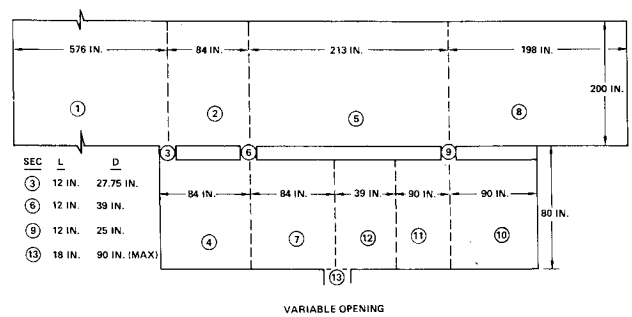

Fig. 11 Multiple compartments with partition vents.

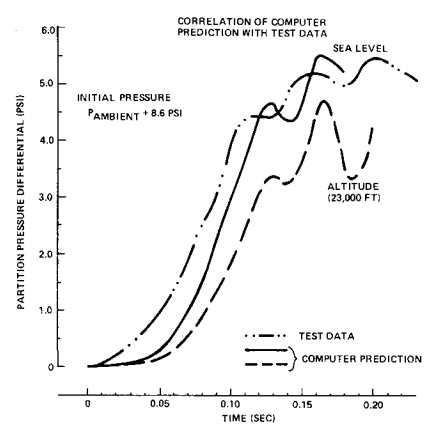

Fig. 12 Partition pressure loading history.

Acknowledgments

The programming was exclusively done by M.J. Smith of the McDonnell Douglas Automation Company (MCAUTO) whose numerous programming innovations made this program possible.

Special thanks are extended to Dr. D.F. Hopkins for the extensive discussions and constructive suggestions in the development of the model.

References

[1] Haloulakos, V.E. and Smith, M.S., "High Frequency Wave Dynamics for Compressible Flow Networks," McDonnell Douglas Astronautics Company, Huntington Beach, Calif., MDC G4874, Aug. 1973.